



Seismic risk evaluation of highway tunnel groups

Pablo Cartes¹ · Alondra Chamorro^{2,3} · Tomás Echaveguren^{1,3}

Received: 1 September 2019 / Accepted: 23 April 2021 / Published online: 12 May 2021
© The Author(s), under exclusive licence to Springer Nature B.V. 2021

Abstract

Tunnels allow the continuity of rural road and urban transportation networks. Their shut-down provokes a loss in the transport system's level service, which entails higher road user costs. Earthquakes are the hazard that most affect the tunnels' serviceability. Depending on the structural damage's magnitude, the serviceability loss can be at different degrees, from marginal changes in traffic flow, associated with minor damages, to traffic interruption, associated with collapsing. Because of seismic phenomena's randomness nature, its effect on tunnel serviceability is estimated in probabilistic terms. Traffic interruption probability was estimated using fragility curves, representing the probability of achieving a specific damage state regarding the seismic hazard intensity. The calibration of tunnel fragility curves requires large samples of damages, seismic intensities, and geological and constructive data, which are not always available, especially in countries with a small number of tunnels in their road network. This work proposes a simplified procedure for evaluating the tunnels' traffic interruption probability due to earthquakes. The approach proposed uses existent seismic exposures maps, a strategy for selecting from existing fragility curves the more suitable, and a simple method to estimate the traffic interruption probability. The procedure analysed 20 tunnels affected by the Maule earthquake in Chile. These tunnels experimented PGA between 0.12 and 0.36 g. The highest risk values were obtained in tunnels without alternative routes and high repairing costs.

Keywords Highway tunnels · Seismic hazard · Risk · Traffic interruption probability

✉ Tomás Echaveguren
techaveg@udec.cl

¹ Civil Engineering Department, Engineering Faculty, Universidad de Concepción, Edmundo Larenas 219, Concepción, Chile

² Construction Engineering and Management Department, Engineering Faculty, Pontificia Universidad Católica de Chile, Santiago, Chile

³ Research Center for the Integrated Management of Natural Disasters (CIGIDEN), ANID/FONDAP/15110017, Vicuña Mackenna, 4860 Santiago, Chile

1 Introduction

Tunnels give continuity to road networks placed in mountainous lands and to urban transportation networks. In rural areas, tunnels are an alternative to large, sinuous, and complex geometrical routes that can compromise drivers' safety, the traffic of vehicles, and the roads' level of service. In urban areas, tunnels serve to subway networks and underground freeways that pass through the cities. Tunnels are classified into drilled/bored, cut and cover, and immersed. Drilled/bored tunnels are built by directly boring the soil, either bare rock or lined with concrete or other materials. Cut-and-cover tunnels are structures generally made of reinforced concrete, with a rectangular section bored in the ground and then roofed with structural elements. Immersed are those excavated in soil strata below water bodies (Argyroudis et al. 2019).

A tunnel's total or partial lack of serviceability increases the operational costs of the transport system. This lack of serviceability can be due to human causes (e.g. traffic accidents, fires, or failures in the maintenance systems) or natural ones (e.g. landslides, seismic structural failures, underground water leakage, or deformations caused by geological faults). Structural or functional causes can also impair serviceability. The former refers to the loss of structural integrity by physical damage to the structure, preventing safe traffic. The latter occurs when the damage level does not affect the structure's stability and integrity but prevents or limits vehicle traffic (Werner et al. 2006). The seismic activity is the main cause for tunnels losing their serviceability since it is a precursor of ground failures, liquefaction, or deformation that can affect the overall structure, the ventilation systems, and lining pavements or access portals (Wang and Zhang 2013; Roy and Sarkar 2017). The damage level and the probability of tunnel traffic interruption because of earthquakes depend on the interaction between the tunnels' structural properties, the soil properties, and the magnitude and propagation of the seismic event (Fabozzi et al. 2018). Therefore, the tunnel management must consider procedures to evaluate traffic interruption scenarios induced by seismic events and adopt cost-efficient mitigation measures that guarantee the road network's operational continuity.

Risk assessment offers a relevant tool for road managers to identify vulnerable segments in the road networks and estimate the probability and consequences of traffic interruptions induced by natural events (Argyroudis et al. 2019, 2020). The risk is estimated in terms of the occurrence probability of a natural event, the asset vulnerability, and the transport system's losses due to the interruption of one or more network links (D'Andrea et al. 2005). The system's losses are estimated in terms of the infrastructure recovery costs and travel time increase due to traffic re-routing (Deco et al. 2013; Selva et al. 2013; Argyroudis et al. 2019; Akiyama et al. 2020).

The tunnel's seismic vulnerability is calculated from fragility curves, which estimate the probability that a tunnel reaches a specific damage state, given the earthquake's intensity. The damage states group together the individual damages experienced by each component of the tunnel. Damages are obtained from damage reports or numerical simulations. In the first case, damages are grouped according to their magnitude and severity. In the second case, damages are grouped according to damage indexes. Argyroudis and Pitilakis (2012) proposed a damage index as the ratio between the actual bending moment of the tunnel cross section and the bending capacity to overcome the lack of indexes to characterize tunnels' damage states. Andreotti (2019) proposed a similar damage index based on the cumulated damage measured through the relative difference between actual rotation and the ultimate plastic rotation.

Literature provided fragility curves of tunnels. Most are calibrated using data from tunnels affected by earthquakes (ALA 2001; Corigliano et al. 2007) and a combination of seismic records and numerical modelling (Huang et al. 2017, 2020; Qiu et al. 2018).

Strong earthquakes are uncommon events, and if the number of tunnels within the road networks is small, the existence of enough empirical evidence concerning the damage gains relevance. In countries with few tunnels exposed to seismic hazards, there are not always enough data of damages, geological and soil characteristics to perform an empirical or analytical calibration of fragility curves; consequently, it is not easy to estimate the vulnerability of tunnels. Likewise, inventory, repairing cost, and traffic data are not always available to estimate repairing and traffic re-routing costs.

The paper presents a simplified procedure to assess the seismic risk of highway tunnels. The method allows identifying and ranking the critical tunnels based on the risk, using existent shake maps and fragility curves to estimate vulnerability. Existing shake maps, such as those provided by the U.S. Geological Survey, can be used to estimate the earthquake intensity. The fragility curves were selected using the Rossetto et al. (2014) procedure for existing fragility curves. Considering the shake map and the fragility curves selected, the traffic interruption probability is estimated. The procedure was applied in Chile to identify the critical tunnels affected by the Maule earthquake.

2 Background on seismic risk assessment of tunnels

The risk is estimated by multiplying the hazard occurrence probability by the system's physical and operational consequences. According to the above definition, the seismic risk in tunnels corresponds to a seismic event's occurrence probability, multiplied by its vulnerability and the consequences on the road network (Nazari and Bargi 2012). Seismic events are described by recurrence models, attenuation models, and shake maps (Vanuvamalai et al. 2018). The vulnerability is obtained from fragility curves, in terms of the tunnels' damage after an earthquake grouped into damage states, given the seismic event's intensity (Kennedy et al. 1980; Choun and Elnashai 2010). The road network consequences are estimated in terms of repair costs, duration of repairs, and additional travel time costs due to re-routing traffic. The possibility of re-routing depends on the level of damage experienced by the tunnel and the existence of alternative links.

2.1 Earthquake-induced damages in tunnels

The damage induced by earthquakes in tunnels allows defining the damage states and, at the same time, damage states are essential to calibrate fragility curves and to estimate vulnerability. Tunnels' seismic damages are caused by ground failure, which depends on the site's geological and geotechnical characteristics, the displacement of active faults, and the ground shaking or vibrations because of the earthquake (Dowding and Rozen 1978). Its magnitude depends on the earthquake's intensity and localization; the tunnel characteristics (geometry, design, construction, and condition); and the characteristics of the site (adverse geology, depth, presence of faults, susceptible to slope sliding) (D'Andrea et al. 2005; Wang and Zhang 2013). Table 1 summarizes a damage classification based on Wang et al. (2001), Asakura et al. (2007), Chen et al. (2012), Roy and Sarkar (2017), and Zhang et al. (2018).

Table 1 Damage classification in tunnels affected by earthquakes

Tunnel component	Damage	Wang et al. (2001)	Asakura et al. (2007)	Chen et al. (2012)	Roy and Sarkar (2017)	Zhang et al. (2018)
Tunnel	Collapse	X		X		X
	Ring breakage					X
Portal	Wall fracture	X		X		
	Access blockage	X				
	Joint cracking	X	X			X
	Wall cracking	X	X			
	Invert uplift					
Liner	Longitudinal cracks	X	X	X	X	X
	Transverse cracks	X	X	X	X	X
	Inclined cracks	X		X	X	X
	Shear failure	X	X	X		X
	Lining spalling	X	X			X
Wall	Water leakage	X		X		X
	Displacement			X		
Pavement	Cracking	X		X	X	X
	Invert uplift		X			

2.2 Damage states

A damage state consists of a grouping of different damages (each of a determined magnitude) experienced by various tunnel components. It makes it possible to characterize the tunnel's overall condition, provide information to calibrate fragility curves, and assess the tunnel's residual serviceability.

Dowding and Rozen (1978) proposed the damage levels “no damage”, “minor”, and “severe” using damage and PGA data from 71 tunnels affected by earthquakes with Richter magnitudes between 5.8 and 8.3, occurring between 1906 and 1971 in California, Alaska, and Japan. The authors concluded that nondamaged tunnels experienced PGA values lower than 0.2 g and that tunnels with a “severe” damage state experienced PGA values greater than 0.5 g. Sharma and Judd (1991) proposed the damage levels “severe”, “moderate”, “slight”, and “no damage” from 192 damage reports from 92 earthquakes. To group the damage states at each level, the authors used the criteria: tunnel depth, type of rock, internal support, geographic location, Richter magnitude, and epicentral distance of each earthquake.

Wang et al. (2001) proposed four damage states following the criteria of crack length (L) and width (W): “no damage” (no damage is detected by visual inspection; regular traffic is allowed); “slight” (slight damage is seen by visual inspection $L < 5$ m and $W < 3$ mm; regular traffic is permitted); “moderate” ($L > 5$ m and $W > 3$ mm; differential displacements due to deep cracks and exposed reinforcements, water leakage, and joint gaps; regular traffic with restrictions is allowed); and “severe” (liquefaction and slope sliding, structural lining collapse, floods, damage in the ventilation and lighting systems; traffic is interrupted).

Werner et al. (2006) proposed four damage states and a qualitative description as follows: “slight/minor” (minor cracking in the lining, slight settlement of ground in portals and small rockfalls in portals; full serviceability is attained after four days), “moderate”

(moderate lining cracking and rockfalls in the portal; complete serviceability is attained after eleven days), and “major” (major lining cracking, and significant settlements in portals; full serviceability is attained after 30 days; before this time traffic should be re-routed).

Xiaoqing et al. (2008) prepared a damage state econometric model with data from 34 tunnels. They considered the same damage descriptors as Sharma and Judd (1991) and added tunnel length, geological faults, age of the tunnel, fortification level, and portals stability.

FEMA (2011) added to the Werner et al. (2006) damage states a fourth damage state and updated the traffic opening as follows: “slight/minor” (minor cracking in the lining, slight settlement of ground in portals, and small rockfalls in portals; full serviceability is attained after three days), “moderate” (moderate lining cracking and rockfalls in the portal; full serviceability is attained after seven days), “extensive” (major lining cracking, and significant settlements in portals; full serviceability is achieved after 90 days), and “complete” (major lining cracking with possible collapse; restoration period is higher than one year; traffic should be re-routed).

Wang and Zhang (2013) proposed tunnel damage states based on earthquake observations in Taiwan, Japan, and China. They extended the classification of Wang et al. (2001) to five damage states (“no damage”, slight, “moderate”, “severe”, and “collapse”). They proposed additional damage thresholds for “moderate” ($3\text{ mm} < W < 30\text{ mm}$ and $5\text{ m} < L < 10\text{ m}$; traffic is allowed) and “severe” ($W > 30\text{ mm}$, $L < 10\text{ m}$, lining displacements over 20 cm and pavement blowup over 20 cm; traffic is not allowed) damage states.

2.3 Fragility curves of tunnels

Fragility curves estimate the probability of exceeding a damage state, given a certain intensity of a natural event. The fragility curves of Fig. 1 allow determining the likelihood that a “Ds” damage on the tunnel exceeds a specific “ds” damage state, given a particular PGA value.

Fragility curves are calibrated using analytical, empirical, expert opinion, or hybrid approaches (Choun and Elnashai 2010). In the analytical approach, damages are estimated by structural and geotechnical modelling combined with real structural tunnel

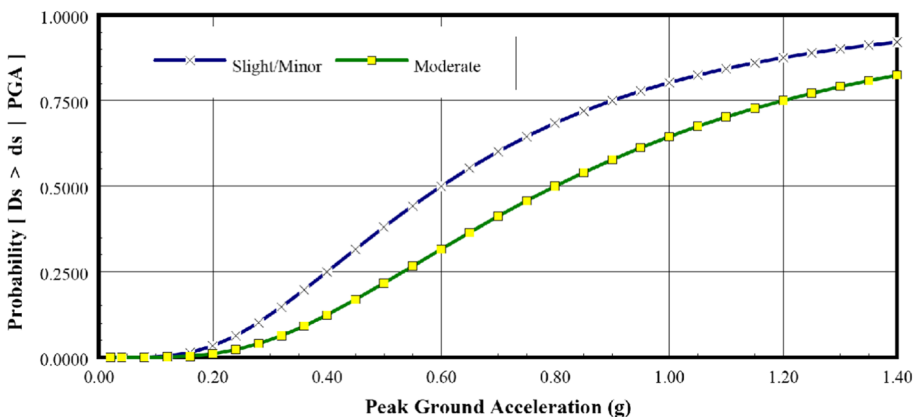


Fig. 1 Example of fragility curves for bored tunnels (FEMA 2011)

responses under accelerations obtained from real seismic responses (Argyroudis and Pitilakis 2012; Argyroudis et al. 2014a, b; Andreotti and Lai 2015; Qiu et al. 2018). The empirical approach uses historical tunnel damage records from different earthquakes and on-site identification of damage states using visual inspection protocols (Corigliano et al. 2007; Le and Huh, 2014). The expert opinion approach estimates subjective probabilities obtained by an expert panel and damage data for building fragility curves (FEMA 2011). It is used when the empirical information is scarce or analytical modeling is intricate (Rossetto et al. 2014). The hybrid approach compensates the lack of data and expert opinions' subjectivity combining analytical and empirical methods.

Equation 1 shows the general model of a fragility curve. It expresses the probability that a damage state “Ds” exceeds the pre-established damage state d_s due to an earthquake of intensity “A”, measured in terms of acceleration.

$$Pf(Ds \geq d_s|A) = \Phi \left[\frac{\ln(A) - \ln(A_{mi})}{\beta_{tot}} \right]; \beta_{tot} = \sqrt{\sum_j \beta_j^2}. \quad (1)$$

It assumes that the distribution of the mean ground acceleration “A”, where the tunnel reaches the damage state threshold d_{s_i} , is a log-normal distribution. The damage threshold (A_{mi}) is the mean value of the peak ground acceleration, where the tunnel reaches a specific damage state. The probability is calculated by a standard cumulative distribution function (Φ) normalized by the overall standard deviation (β_{tot}). The overall standard deviation is estimated under the assumption that their components (β_j) are statistically independent. In analytical and hybrid calibration approaches, the components of β_{tot} included the uncertainty in the seismic demand (seismic records dispersion, attenuation laws, and the selection of the seismic demand variable), in the structural capacity (mechanics and geometric parameters of tunnels, structural characteristics) in the damage state thresholds and in the type of method used to calibrate the fragility curve (Rossetto et al. 2014; Argyroudis et al. 2019). Shinozuka et al. (2000) suggest estimating the confidence interval of the fragility curves' parameters to obtain the calibration's uncertainty.

Table 2 shows the fragility curves available in the literature, calibrated for different tunnel configurations, intensity measures, soil conditions, and construction qualities.

The following characteristics of input data are identified in the models of Table 2:

- (a) Type of tunnel: fragility curves are specific to each type of tunnel. There are different fragility curves for bored/drilled, cut and cover, and reinforced concrete box tunnels.
- (b) Construction quality: only models #1 and #8 consider construction quality. Other models assume good construct quality.
- (c) Hazard intensity measure: most models use PGA and PGV as measures of hazard intensity. Model #11 uses Arias' intensity, and model #13 uses PSA.
- (d) Tunnel depth: models #1 and #6 consider tunnels depth between 20 and 330 m. Model #17 uses tunnels depths of 10, 15, 20, and 25 m. Model #16 uses tunnels depths of 80, 200, 300, and 400 m. Other models considered depths between 4 and 44 m. Tunnel cross section: most models used circular cross sections with diameters of 6, 9, and 10 m. Only models #11 and #13 propose fragility curves dependent on diameter.
- (e) Tunnel age: the tunnel age is considered only in models #4 and #14 regarding resistance degradation because of reinforcement corrosion. These fragility curves include tunnels age of 0, 50, 75, and 100 years.

Table 2 Fragility curves available in the literature

#	Author	Type of tunnel	Damage states	Hazard intensity variable	Ground motions	Calibration procedure
1	ALA (2001)	Bored/drilled, cut-and-cover tunnels classified by construction quality	Minor/moderate /heavy	PGA < 1.1 g	10 Ground motions (Mw < 8.4)	Empirical
2	Andreotti and Lai (2015)	Bored circular tunnel with reinforced lining	Minor/moderate/extensive	PGV < 2 m/s	11 Signals from accelerograph	Semi-analytical
3	Argyroudis and Pitilakis (2012)	Bored, cut and cover	Minor/moderate/extensive	PGA < 1.6 g	9 Ground motions of Eurocode 8 database (Mw < 7.4)	Semi-analytical
4	Argyroudis and Kaynia (2014)	Bored circular tunnel with reinforced lining	Minor/moderate/extensive	PGA < 1.4 g	6 Ground motions of Eurocode 8 database (Mw < 7.4)	Semi-analytical
5	Avanaki et al. (2018)	Bored circular tunnel with reinforced lining	Minor/moderate/extensive	PGA < 2.0 g	20 Ground motions of PEER database (Mw < 7.5)	Semi-analytical
6	Corigliano et al. (2007)	Not available	Slight/moderate	PGV < 120 cm/s	Attenuation model and rupture distance from recent earthquakes with damaged tunnels	Empirical
7	Codermatz et al. (2003)	Bored, cut and cover	Not available	PGA < 1.0 g	Attenuation model calibrated for Italy	Adopted from Hazus
8	FEMA (2011)	Bored/drilled, cut and cover	Slight/moderate/extensive	PGA < 1.4 g PGD < 48 in (120 cm)	Not available	Not available
9	Le et al. (2014)	Double box reinforced concrete	Minor/moderate/extensive	PGA < 0.45 g	Design response spectrum	Analytical
10	Nguyen et al. (2019)	Single, double, triple box reinforced concrete for subway	Minor/moderate/extensive	PGA < 1.5 g PGV < 1 m/s PGV/ ₃₀ < 0.005	20 Ground motions of PEER database (Mw < 7.8)	Semi-analytical
11	Huang et al. (2017)	Bored circular tunnel	Minor/moderate/extensive	Arias Intensity < 5 m/s Ground Arias intensity < 10 m/s	40 Ground motions of PEER database (Mw < 7.3)	Semi-analytical

Table 2 (continued)

#	Author	Type of tunnel	Damage states	Hazard intensity variable	Ground motions	Calibration procedure
12	Osmi and Ahmad (2016)	Bored circular tunnel with reinforced lining	Minor/moderate/extensive	PGA < 1.8 g	5 Ground motions of PEER database (Mw not reported)	Semi-analytical
13	Qiu et al. (2018)	Bored circular tunnel	Minor/moderate/extensive	PSA < 3.0 g	100 Ground motions of PEER database (Mw < 7.3)	Semi-analytical
14	Argyroudis et al. (2017)	Bored circular tunnel with reinforced lining	None/minor/moderate/extensive/complete	PGA < 1.4 g	6 Ground motions records (Mw < 7.4)	Semi-analytical
15	Park et al. (2019)	Double box reinforced concrete for subway	Minor/moderate/extensive	PGA < 1.5 g, PGV/ $V_{s,30}$ < 0.005	Design response spectrum	Analytical
16	Andreotti (2019)	Bored circular tunnel	Slight/moderate /extensive	PGV < 1.8 m/s PGA < 1.8 g Buried deep between 80 and 400 m	Simulated ground motions	Analytical
17	Hu et al. (2020)	Bored circular tunnel with reinforced lining	Minor/moderate /extensive	PGA < 1.6 g Buried deep between 10 and 35 m	15 Ground motions of PEER database (Mw < 7.6)	Semi-analytical
18	Huang et al. (2020)	Bored circular tunnel with reinforced lining for subway	None/minor/moderate/extensive/complete	PGV < 1.6 m/s PGA < 1.6 g Buried deep between 9 and 30 m	12 Ground motions records of PEER database (Mw < 7.36)	Semi-analytical
19	De Silva et al. (2020)	Bored circular tunnel with reinforced lining for subway	Not used	PGV < 2.0 m/s PGA < 1.6 g Buried deep between 10 and 25 m	10 Ground motions of PEER database (Mw < 7.4)	Semi-analytical

- (f) **Damage states:** most models use three or four damage states. The criteria for defining damage states depend on the calibration method. In the empirical fragility curves, damage states are determined using damage reports from past earthquakes. In analytical or semi-analytical fragility curves, the damage states are defined by damage indices calculated by numerical simulation as the ratio between the actual and capacity bending moment of the tunnel cross-section. Models #2 and #16 use a damage index based on the cumulative plastic rotation. In model #5, the damage index combines lining strains with bending moment. The rotation, strains, and moments are obtained by structural modelling.
- (g) **Soil conditions:** it is considered through a single homogeneous soil layer (for instance, models #9, #10, and #13); a single fragility curve for different soil layers (for instance, model #15); and fragility curves for different soil types (for instance models #3, #4, #14 and #18). Model #16 considers the rock quality according to its geotechnical characteristics.

A critical aspect of calibrating fragility curves is the data availability, in both quantity and quality, concerning seismic events and damages experienced by tunnels obtained through systematic protocols. It is crucial in countries with a few tunnels in their road network or does not rely on maintenance management systems that systematically collect data to calibrate fragility curves (Selva et al. 2013). If there are no locally calibrated fragility curves, an alternative is to select the most suitable ones from a set of existing curves. However, inter-model variability is a practical difficulty that needs to be addressed. To this end, Shinozuka et al. (2000), Selva et al. (2013), and Rossetto et al. (2014) discuss procedures for selecting a fragility curve from existing curves.

Shinozuka et al. (2000) proposed a statistical procedure to combine bridge fragility curves. They establish that a combined fragility curve is the weighted sum of class “i” bridge fragility curves. The weights represent the proportion of class “i” bridges in the total population of bridges in the road network. They also warn that the combined curve’s total variance increases concerning the sum of the variances of each bridge class’s fragility curves. Selva et al. (2013) used a Bayesian approach to show the propagation of inter-model variability of fragility curves in loss functions.

Rossetto et al. (2014) propose a systematic procedure for selecting a suitable fragility curve, which discriminates between analytical and empirical curves and then classifies them according to their relevance and quality. The relevance criterion depends on each fragility curve’s ability to represent an asset’s damage states for a given range of hazard intensities. The quality criterion considers the quality of the input data, the rationality of the model (in terms of uncertainty and modelling approach), and the quality of the technical documentation used to calibrate the curves.

3 Procedure for tunnel risk assessment

The risk estimation procedure is organized into three steps: (1) hazard analysis, (2) vulnerability assessment, and (3) risk estimation (Fig. 2). The seismic scenario is configured in the first step, considering the earthquake’s location and magnitude, thereby obtaining seismic exposure maps to which the tunnels’ geolocation is superimposed. These maps allow determining seismic intensities values for each tunnel, such as peak ground displacements, velocities, or accelerations, among others. The second step determines suitable fragility

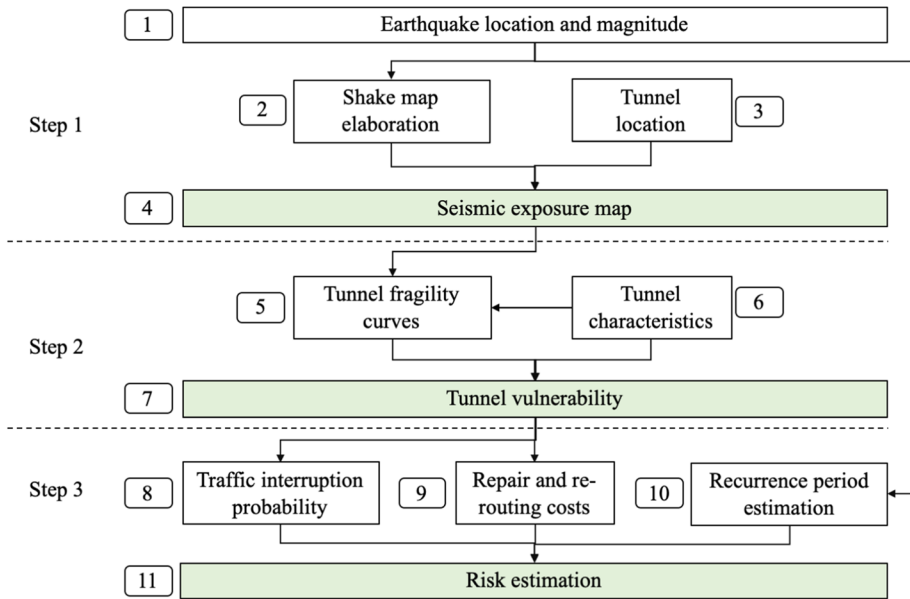


Fig. 2 Proposed method for risk assessment of highway tunnels

curves for each tunnel, based on their characteristics (tunnel type and construction quality). From fragility curves, the vulnerability of tunnels is obtained. In the third step, the risk is estimated considering the seismic recurrence, the tunnel vulnerability, and the cost. Costs include repair costs and travel time cost increasing due to the re-routing of traffic during repairs.

3.1 Tunnel seismic exposure maps

This map requires the location and moment magnitude of the earthquake and the geolocation of highway tunnels. Existing exposure maps, such as those provided by the U.S.G.S. (Shedlock and Tanner 1999), are needed. The seismic intensity values in a specific location can also be estimated with acceleration attenuation models locally calibrated, but this type of model is intensive in input data. Afterwards, the exposure maps and georeferenced tunnels are superimposed, thus obtaining the seismic intensity value for each tunnel.

3.2 Estimate of the tunnel vulnerability

This stage infers the tunnel vulnerability based on the fragility curves. Three input data are required: (a) the seismic hazard map of the tunnels; (b) the inventory of georeferenced tunnels; and (c) tunnel fragility curves. The tunnels' seismic hazard map is obtained from step 1 (Fig. 2). The inventory of tunnels is obtained directly on-site or from existing inventories and includes the following:

- Location of each tunnel by georeferencing their portals.
- Type of tunnel: bored in hard rock (bored/drilled) or covered trench (cut and cover).

- General tunnel construction characteristics: portal, liner, and construction age.
- Construction quality, according to ALA (2001):
- Tunnel bored with poor-to-average construction quality: tunnels with poor-to-average quality rock, without lining, with treated wood or masonry lining, with nonreinforced or low-strength concrete.
- Tunnel bored with good construction quality: tunnels in hard rock, designed for specific geological conditions (special supports or reinforced lining in weak areas), with nonreinforced lining and good strength concrete. It also includes a reinforced lining.
- Cut-and-cover tunnel with poor-to-average construction quality: tunnels with a lining of treated wood, masonry, or nonreinforced concrete. Includes tunnels that were not designed to withstand excessive strains.
- Cut-and-cover tunnel with good construction quality: tunnels designed for seismic load, excessive strain, with reinforced concrete lining.

The fragility curves are selected in three steps: first, to collect existent fragility curves based on the same seismic intensity measure; second, to choose fragility curves calibrated for similar conditions of the place in which will be applied; and third, to use the evaluation criteria set out by Rossetto et al. (2014) to select the proper fragility curve. The criteria of Rossetto et al. (2014) are shown in Fig. 3.

Each criterion is assessed based on three scores: “high” (score 3), “medium” (score 2), and “low” (score 1). The final score is the sum of these qualifications for each sub-criterion. The curve with the highest final score is selected. When there is more than one fragility curve with the highest score, they are combined through Eq. 2, where “ n ” is the number of fragility curves, $P_j()$ is each fragility curve, and $E[P()]$ is the combination of fragility curves.

$$E[P(DS \geq dsi|A)] = \sum_{j=1}^n w_j P_j(DS \geq dsi|A). \tag{2}$$

The weighted factor w_j represents the probability that the fragility curve is the true one among the “ n ” curves to be combined. It can be obtained by assigning the same weight to

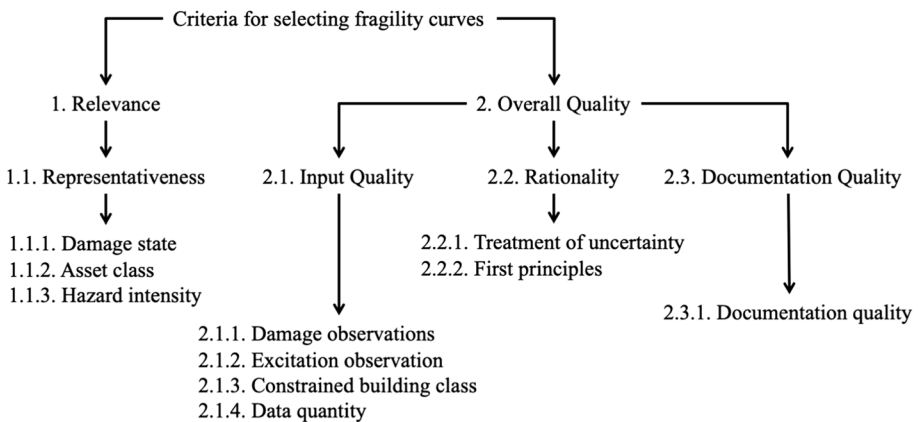


Fig. 3 Criteria for selecting fragility functions. Adapted from Rossetto et al. (2014)

each curve, which is equivalent to the inverse of the total curves to be combined, weighting by the score corresponding to the overall quality criterion of the curves, considering the representativeness and reliability of each curve or through the opinion of experts (Scherbaum et al. 2005; Scherbaum and Kuehn 2011; Rossetto et al. 2014). From the selected fragility curve, vulnerability is obtained using the discrete probabilities between damage states.

3.3 Risk estimation

The risk is estimated by multiplying the earthquake's recurrence period with the traffic interruption probability and the total cost. The earthquake's recurrence period is calculated by models that correlate the earthquake magnitude and the mean annual exceeding events. The traffic interruption probability depends on the damage experienced by the tunnel. Traffic closure rules provide a proxy of this probability for each damage state. According to Wang and Zhang (2013), the following closure rules were proposed: in the damage states, "none" traffic is allowed, and the travel time increase is zero. In the damage state "slight", the tunnel is closed for two hours during the inspection, cleaning, and systems verification. All the traffic is re-routed for two hours. For the damage state "moderate", traffic is re-routed during minor repairs (two or three days). In other damage states, traffic is not permitted and is re-routed. Reconstruction time is approximately one year. The total cost is the cost of repair, plus the additional cost of travel time due to re-routing by assuming that there is no long-term modification of the travel matrix involving additional nontrip costs.

4 Case study: risk assessment of Chilean tunnels

4.1 Description of the case study

Chile is in the convergent border between the Nazca and the South American plates; therefore, most earthquakes are due to subduction. In the last 400 years, Chile has registered approximately 20 earthquakes with magnitudes above 7.5. The Valdivia earthquake of 1960 has the highest magnitude ever recorded and reached between 9.6 and 9.8 of the Richter scale. This case study uses the 2010 Maule earthquake data, which impacted Chile from Valparaiso's region to La Araucanía, covering 30% of the Chilean territory. It had a moment magnitude of 8.8 and a rupture length of 500 km offshore, 25 km from the coastline. Chile has 31 bored highway tunnels, with a total of 34.2 km. The lengths vary between 142 and 4,520 m, and the commissioning dates oscillate from 1910 to 2017. Among these tunnels, nine have reinforced concrete lining, 19 have shotcrete, and 3 have no lining; 6 have one lane in both directions, 11 have one lane per direction, 1 has two lanes per direction, and 13 have two lanes in the same direction.

4.2 Drawing up of the seismic hazard map of tunnels

The seismic hazard map was based on the Maule earthquake PGA map, drawn up by the US Geological Survey. The tunnel locations were obtained from the tunnel inventory of the Ministry of Public Works of Chile. Both maps were superimposed to identify the 31 highway tunnels affected by the Maule earthquake. The coherence between each tunnel's construction date and the date of occurrence of the earthquake was checked. Figure 4

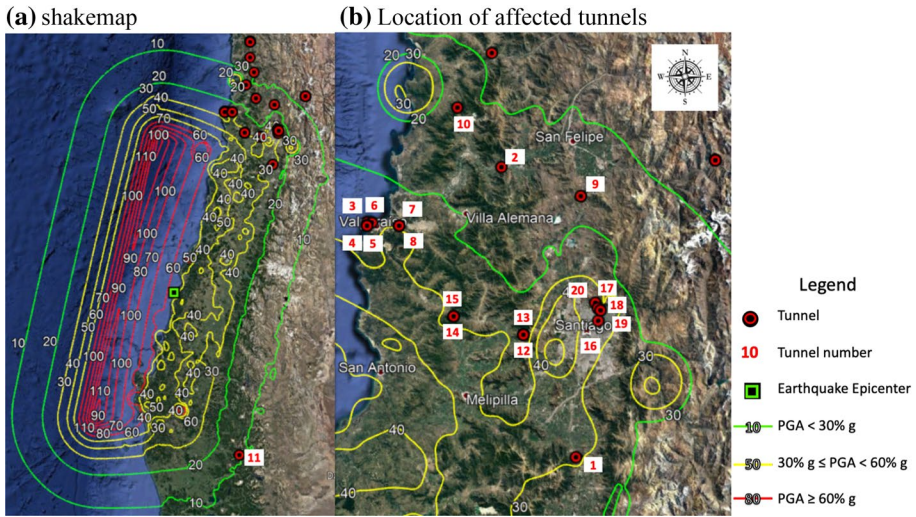


Fig. 4 PGA seismic exposure of tunnels during the Maule earthquake. **a** Shakemap, **b** location of affected tunnels

shows the PGA map and the 20 tunnels affected by the Maule earthquake (red circles), and Table 3 shows the primary data for each tunnel. All the tunnels are bored/drilled. Tunnels #3 to #8 are in the coastal zone and the others in Chile’s central valley. The rupture distance was higher than 40 km for the nearby tunnels. According to Poulos et al. (2019), Maule’s earthquake’s recurrence period is 242 years.

4.3 Determination of the expected damage level

Figure 5 consolidates the frequency at which the 20 tunnels of Table 3 experienced different acceleration ranges during the Maule earthquake. In two cases, 20% of the time, a tunnel experienced an acceleration below 0.2 g; 80% of the time (16 cases), a tunnel experienced an acceleration between 0.2 and 0.4 g; no tunnel experienced an acceleration equal or higher than 0.4 g. It means that 20% of the tunnels should not have suffered any damage and that the remaining 80% suffered moderate damage and, therefore, none of them should have lost their serviceability. The lack of post-earthquake damage data did not allow comparing the reliability of the Dowding and Rozen (1978) thresholds, which helped to elaborate Fig. 5.

Reports concerning the transport infrastructure damage after the Maule earthquake were focused on bridges, roads, buildings, and historical buildings (Elnashai et al. 2010; Yen et al. 2011; Medina et al. 2010), so no specific reports are dealing with the tunnels’ behaviour that allows accurately determining their damage states. Because Elnashai et al. (2010), Yen et al. (2011), and Medina et al. (2010) did not report tunnel damaged, it was assumed that the damage ranges proposed by Dowding and Rozen (1978) were assimilated to “slight” and “moderate” damage states. The absence of data also prevented using, for example, the central damage index proposed by Argyroudis and Pitilakis (2012) to identify the damage states.

Table 3 Characteristics of Chilean tunnels affected by Maule earthquake

Tunnel #	Name	Length (m)	Traffic opening year	Lining type	Traffic (veh/day-year)	
					Light	Heavy
1	Angostura	347	1949	Nonstructural	27,283	4077
2	La Calavera	298	1950	Nonstructural	50,894	8981
3	La Pólvara 1	2183	2007	Structural	10,229	2095
4	La Pólvara 2	301	2007	Structural	10,229	2095
5	La Pólvara 3	439	2007	Structural	10,229	2095
6	La Pólvara 1-A	165	2007	Nonstructural	5,106	1198
7	Jardín Botánico O	245	1996	Nonstructural	11,408	3033
8	Jardín Botánico P	245	1996	Nonstructural	11,408	3033
9	Chacabuco	2045	1972	Structural	10,350	1,150
10	El Melón	2543	1995	Structural	52,092	7784
11	Las Raíces	428	1939	Without lining	859	152
12	Lo Prado 1	200	1970	Structural	36,040	4454
13	Lo Prado 2	2800	2005	Structural	36,040	4454
14	Zapata 1	1215	1955	Nonstructural	31,570	3902
15	Zapata 2	1215	2004	Nonstructural	31,570	3902
16	San Cristóbal	1808	2008	Nonstructural	26,300	1384
17	Manquehue 1	157	2009	Nonstructural	11,073	112
18	Manquehue 2 left	450	2008	Nonstructural	11,073	112
19	Manquehue 2 right	450	2008	Nonstructural	11,073	112
20	Chamisero 1 left	610	2008	Nonstructural	11,073	112

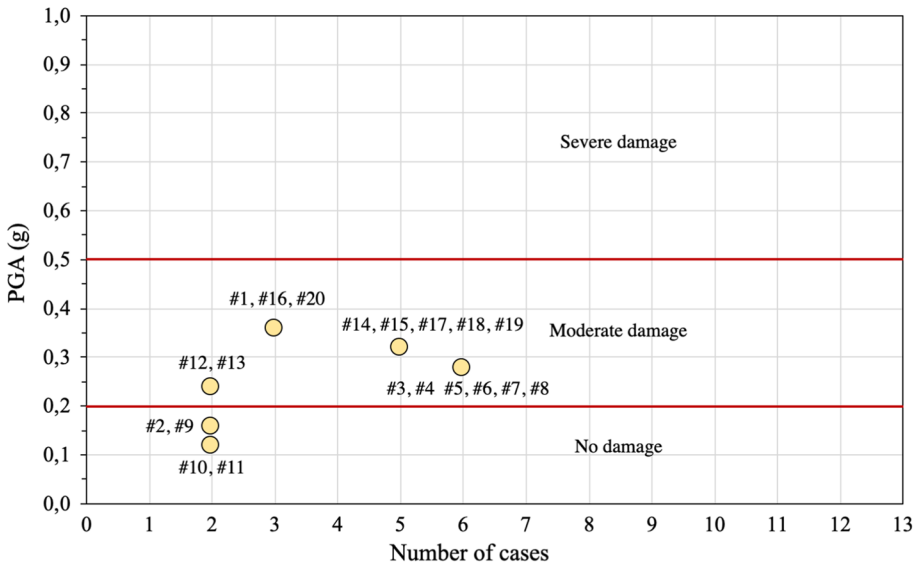


Fig. 5 Expected damage level in Chilean tunnels

4.4 Selection of fragility curves

The first step was to identify the available fragility curves of tunnels from the literature. Table 2 shows the fragility curves preliminary identified and their general properties. We eliminate the fragility curves with hazard intensity units different to PGA, those calibrated for box tunnels, those calibrated with design response spectrums, and those based on Eurocode, according to the criteria “asset class” and “hazard intensity” of Fig. 3. The subset of fragility curves were: #1, #5, #8, #12, and #16. The qualification procedure of Fig. 3 was applied to this subset of fragility curves, obtaining the following ranking: #1, #8, #5, #16, and #12. Model #1 scored highest on the relevance criterion, while all other models scored slightly lower. In the general quality criterion, model #1 obtained a higher score than the rest of the models mainly because it considers a substantially higher number of seismic events than the rest of the models. Therefore, according to the criteria in Fig. 3, model #1 was selected to estimate the tunnel’s vulnerability.

Figure 6 summarizes the fragility curves recommended for Chile, according to the following damage states and construction qualities: (a) tunnels bored in rocks, poor-to-average construction quality for slight damage (1L), and moderate damage (1 M); (b) tunnels bored in rock, good construction quality for slight (2L) and moderate damage (2 M). These fragility curves were used to estimate the probability that the Maule earthquake’s tunnels exceeded the “slight” and “moderate” damage states.

Table 4 shows that PGA ranges that tunnels experienced during the Maule earthquake fluctuated between 0.12 and 0.36 g. For this PGA range, the exceedance probability varies between 0.02 and 0.50 for the “slight” damage state and between 0.00 and 0.13 for the “moderate” damage state (poor-to-average constructive quality); between 0.02 and 0.08 for the “slight” damage state and between 0.00 and 0.02 for the “moderate” damage state (good constructive quality). Table 4 also shows the discrete probabilities associated with the damage states “slight”, “moderate”, and “no damage”.

4.5 Risk estimation

The risk was estimated for the 20 tunnels affected by the Maule earthquake. The Poulos et al. (2019) model was used to estimate the Maule earthquake’s recurrence period.

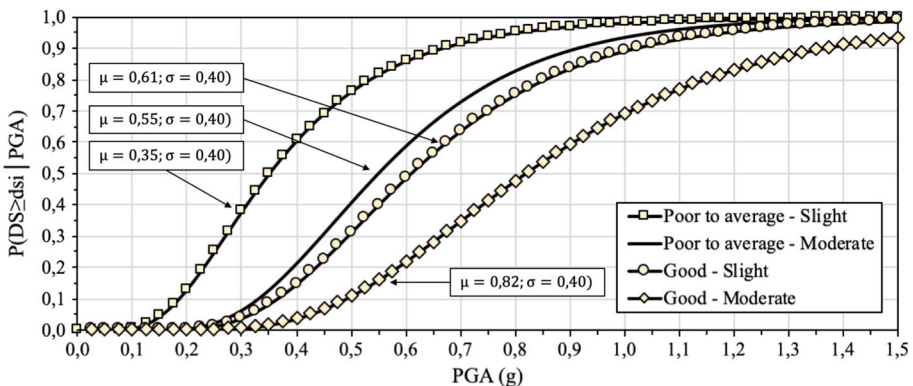


Fig. 6 Tunnel fragility curves proposed for Chile

Table 4 Exceedance and traffic interruption probabilities of Chilean tunnels

Tunnel #	Lining type	Constructive quality	PGA (g)	Exceedance probabilities		Discrete probabilities		
				Slight	Moderate	No damage	Slight	Moderate
1	Nonstructural	Poor-to-average	0.36	0.53	0.15	0.47	0.38	0.15
2	Nonstructural	Poor-to-average	0.16	0.06	0.00	0.94	0.06	0.00
3	Structural	Good	0.28	0.02	0.00	0.98	0.02	0.00
4	Structural	Good	0.28	0.02	0.00	0.98	0.02	0.00
5	Structural	Good	0.28	0.02	0.00	0.98	0.02	0.00
6	Nonstructural	Poor-to-average	0.28	0.02	0.00	0.98	0.02	0.00
7	Nonstructural	Poor-to-average	0.28	0.02	0.00	0.98	0.02	0.00
8	Nonstructural	Poor-to-average	0.28	0.02	0.00	0.98	0.02	0.00
9	Structural	Good	0.16	0.00	0.00	1.00	0.00	0.00
10	Structural	Good	0.12	0.00	0.00	1.00	0.00	0.00
11	Without lining	Poor-to-average	0.12	0.02	0.00	0.98	0.02	0.00
12	Structural	Good	0.24	0.01	0.00	0.99	0.01	0.00
13	Structural	Good	0.24	0.01	0.00	0.99	0.01	0.00
14	Nonstructural	Poor-to-average	0.32	0.44	0.09	0.56	0.35	0.09
15	Nonstructural	Poor-to-average	0.32	0.44	0.09	0.56	0.35	0.09
16	Nonstructural	Poor-to-average	0.36	0.55	0.14	0.45	0.41	0.14
17	Nonstructural	POOR-to-average	0.32	0.44	0.09	0.56	0.35	0.09
18	Nonstructural	Poor-to-average	0.32	0.44	0.09	0.56	0.35	0.09
19	Nonstructural	Poor-to-average	0.32	0.44	0.09	0.56	0.35	0.09
20	Nonstructural	Poor-to-average	0.36	0.55	0.14	0.45	0.41	0.14

The tunnels' vulnerability was calculated from the fragility curves proposed for Chile, according to Fig. 6, and the PGA experienced by tunnels during the Maule earthquake according to Table 4 for each damage state. The tunnel's repairing cost was estimated using cost data from MOP (2016). The operating cost was estimated using the unit time travel cost obtained from the Chilean Ministry of Social Development and Family (MSDF 2020). The travel time increase was calculated considering the best available route to re-route whether each tunnel is closed, the closure time, and the average travel speed along that route. The tunnel's traffic was obtained using the National Traffic Survey data elaborated yearly by the Ministry of Public Works of Chile (MOP 2018, 2019).

The risk values obtained for each tunnel are summarized in Table 5. The risk in tunnels #1, #14, #15, and #16 is substantially higher than in other tunnels because Tunnel #1 has no alternatives and requires a detour with alternating traffic. In tunnels #14 and #15, the alternative route's standard is lower than the standard of the tunnels' route. The alternative route is bi-directional, sinuous, and with steep slopes, reducing traffic speed and increasing travel time. In tunnel #16, the alternative route is of a similar standard but passes through urban areas with high traffic, so the traffic re-routed increases travel times.

Table 5 Risk values calculated for each tunnel

Tunnel #	Traffic (vehicles/day-year)			Probability of traffic interruption		Total cost (mUS\$)			Risk (mUS\$)		
				Slight	Moderate				Slight	Moderate	
	Light	Heavy		Slight	Moderate	Repair	Travel time	Repair	Travel time	Slight	Moderate
1	27,283	4077		0.38	0.15	37	7739	359	40,947	12.2	25.6
2	50,894	8981		0.06	0.00	32	4885	308	30,070	1.2	0.0
3	10,229	2095		0.02	0.00	231	798	3414	5612	0.1	0.0
4	10,229	2095		0.02	0.00	32	798	471	5,612	0.1	0.0
5	10,229	2095		0.02	0.00	47	798	687	5612	0.1	0.0
6	5106	1198		0.02	0.00	17	405	171	3208	0.0	0.0
7	11,408	3033		0.02	0.00	26	2298	253	20,307	0.2	0.0
8	11,408	3033		0.02	0.00	26	2298	253	20,307	0.2	0.0
9	10,350	1150		0.00	0.00	217	13,024	3198	52,364	0.0	0.0
10	52,092	7784		0.00	0.00	270	4925	3977	26,061	0.0	0.0
11	859	152		0.02	0.00	14	198	2717	1219	0.0	0.0
12	36,040	4454		0.01	0.00	297	24,179	4379	107,376	1.0	0.0
13	36,040	4454		0.01	0.00	297	24,179	4379	107,376	1.0	0.0
14	31,570	3902		0.35	0.09	129	31,183	1256	138,477	45.3	52.0
15	31,570	3902		0.35	0.09	129	31,183	1256	138,477	45.3	52.0
16	26,300	1384		0.41	0.14	192	5645	1869	11,122	9.9	7.5
17	11,073	112		0.35	0.09	33	1545	325	599	2.3	0.3
18	11,073	112		0.35	0.09	48	1545	465	599	2.3	0.4
19	11,073	112		0.35	0.09	48	1545	465	599	2.3	0.4
20	11,073	112		0.41	0.14	65	1545	631	599	2.7	0.7

5 Conclusions

The work proposes a simplified procedure to assess highway tunnels' seismic hazards based on damage studies and fragility curves obtained from the international experience. The outcome of the procedure is the traffic interruption probability. The procedure proposed aids road agencies in assessing a group of tunnels' seismic risk and making decisions such as reinforcement or repairing, considering the existence or not of alternative routes to prevent the traffic interruption. From the study conducted, the following was concluded:

After a seismic event, the characterization of damage is a critical task to have high-quality data with which to define damage states. Therefore, it is necessary to have protocols that allow estimating the magnitude and intensity of the damage. However, road agencies do not always have such protocols. Due to the need to enable the tunnels to traffic, the damages survey is not a priority. Consequently, damage data were not always available, reducing the options of calibrating fragility curves and estimating tunnels' seismic vulnerability.

The damage states are determined using the damage magnitudes of the tunnels' various structural components obtained after an earthquake. For example, several authors propose damage states in terms of the width and length of cracks in the lining, exposure of reinforcements, collapse of portals, among others. For this reason, it is essential to have damage survey protocols. When these do not exist, it is not convenient to arbitrarily define damage states, considering that each damage state determines the possibility of restricting or enabling traffic through the tunnels and the restoration period. Without periodic damage reports, it is impossible to define damage states and calibrate fragility curves.

Due to the variability of input data and the diversity of fragility curve calibration considerations, it is not appropriate to arbitrarily use one or more fragility curves to estimate tunnel seismic vulnerability when locally calibrated fragility curves are not available. On the contrary, it is necessary to select fragility curves considering the characteristics of the tunnels of a road network, the type of earthquake, and the geological and soil conditions at the tunnel sites to ensure representativeness for the case study. The selection procedure adopted in the case study provides a systematic tool for a proper selection of fragility curves.

The case study results show that the 20 tunnels within the Maule earthquake area were exposed to PGA between 0.12 and 0.36 g. The vulnerability to "slight" damage is lower than 0.41 and lower than 0.15 for "moderate" damage. The estimation shows that the major losses are associated with the tunnels that combine the highest vulnerabilities and poor alternative routes. These theoretical results are consistent with the evidence obtained on-site by the Chilean Road Department after the Maule earthquake, which revealed that tunnels had not suffered any damage that compromises the serviceability.

One of the case study's limitations was the lack of accurate inventory data and damage reports after the Maule earthquake, so it was difficult to estimate more precisely the actual damage states, the detailed geometry of the tunnels, and their construction quality. Thus, the quality of the available information is a relevant criterion in selecting the fragility curves.

The proposed procedure allows the risk evaluation of groups of road tunnels. Therefore, one of the main challenges is integrating into the risk assessment other road assets, such as bridges and road platforms, and other natural hazards such as floods, landslides, and lahar flows.

Additional research is required to improve the proposed procedure. The main issues are: to calibrate models of seismic event recurrence for assessing several seismic scenarios

instead of a specific earthquake; to estimate the transportation costs considering the effects of earthquakes on the origin–destination travel matrixes; and to estimate more accurately the traffic on the road network.

Acknowledgements The authors thank the National Research and Development Agency (ANID) of Chile for supporting the projects CONICYT/FONDAP/15110017 project “National Research Center for Integrated Natural Disaster Management (CIGIDEN)” and FONDECYT 1181754 “Socio-economic modelling of mitigation strategies for resilient critical infrastructure: application to drink water systems and road networks”, within which this paper was prepared.

References

- Akiyama M, Frangopol D, Ishibashi H (2020) Toward lifecycle reliability-, risk- and resilience-based design and assessment of bridges and bridge networks under independent and interacting hazards: emphasis on earthquake, tsunami and corrosion. *Struct Infrastruct Eng* 16(1–2):26–50. <https://doi.org/10.1080/15732479.2019.1604770>
- ALA (2001) Seismic fragility formulations for water systems, part I Guideline, American Lifelines Alliance, United States
- Andreotti G (2019) Lai CG (2019) Use of fragility curves to assess the seismic vulnerability in the risk analysis of mountain tunnels. *Tunn Undergr Space Technol*. <https://doi.org/10.1016/j.tust.2019.103008>
- Andreotti G, Lai CG (2015) Methodology to derive damage state-dependent fragility curves of underground tunnels. In: 6th International conference on earthquake geotechnical engineering, 1–4 November, Christchurch, New Zealand
- Argyroudis S, Ptilakis KD (2012) Seismic fragility curves of shallow tunnels in alluvial deposits. *Soil Dyn Earthq Eng* 35:1–12. <https://doi.org/10.1016/j.soildyn.2011.11.004>
- Argyroudis S, Kaynia AM (2014) Fragility functions of highway and railway infrastructure. In: Ptilakis K et al (eds) SYNER-G: typology definition and fragility functions for physical elements at seismic risk, geotechnical, geological and earthquake engineering 27. Springer, Dordrecht, pp 299–326
- Argyroudis S, Tsinidis G, Gatti F, Ptilakis KD (2014) Seismic fragility curves of shallow tunnels considering SSI and aging effects. In: 2nd Eastern European tunneling conference, 28 Sep–1 Oct, Athens, Greece
- Argyroudis S, Tsinidis G, Gatti F, Ptilakis KD (2017) Effects of SSI and lining corrosion on the seismic vulnerability of shallow circular tunnels. *Soil Dyn Earthq Eng* 98:244–256. <https://doi.org/10.1016/j.soildyn.2017.04.016>
- Argyroudis S, Mitoulis SA, Winter M, Kaynia AM (2019) Fragility of transport assets exposed to multiple hazards: state-of-the-art review toward infrastructural resilience. *Reliab Eng Syst Saf*. <https://doi.org/10.1016/j.res.2019.106567>
- Argyroudis S, Mitoulis SA, Hofer LZ (2020) Resilience assessment framework for critical infrastructure in a multi-hazard environment: case study on transport assets. *Sci Total Environ* 714(2020):1–20. <https://doi.org/10.1016/j.scitotenv.2020.136854>
- Asakura T, Tsukada K, Matsunaga T, Matsuoka S, Yashiro K, Shiba Y, Oya T (2007) Damage to mountain tunnels by earthquake and its mechanism. In: 11th International society for rock mechanics and rock engineering congress, 9–13 July, Portugal
- Avanaki MH, Hoseini A, Vahdani S, de Santos C (2018) Seismic fragility curves for vulnerability assessment of steel fiber reinforced concrete segmental tunnel linings. *Tunn Undergr Space Technol* 78(2018):259–274. <https://doi.org/10.1016/j.tust.2018.04.032>
- Chen CH, Wang TT, Jeng FS, Huang TH (2012) Mechanisms causing seismic damage of tunnels at different depths. *Tunn Undergr Space Technol* 28:31–40
- Choun YS, Elnashai AS (2010) A simplified framework for probabilistic earthquake loss estimation. *Probab Eng Mech* 25(4):355–364. <https://doi.org/10.1016/j.probengmech.2010.04.001>
- Codermatz R, Nicolich R, NSlejko D (2003) Seismic risk assessments and GIS technology: applications to infrastructures in the Friuli-Venezia Giulia region (NE Italy). *Earthq Eng Struct Dyn* 32:1677–1690. <https://doi.org/10.1002/eqe.294>
- Corigliano M, Lai CG, Barla G (2007) Seismic vulnerability of rock tunnels using fragility curves. In: Ribeiro e Sousa L, Olalla C, Grossmann N (eds) 11th Congress of the international society for rock mechanics, Taylor and Francis, London, pp 1173–1176

- D'Andrea A, Cafiso S, Condorelli A (2005) Methodological considerations for the evaluation of seismic risk on road network. *Pure Appl Geophys* 162(2005):767–782. <https://doi.org/10.1007/s00024-004-2640-0>
- De Silva F, Fabozzi S, Nikitas N, Bilotta E, Fuentes R (2020) Seismic vulnerability of circular tunnels in sand. *Géotechnique*. <https://doi.org/10.1680/jgeot.19.SiP.024>
- Decò A, Bochini P, Frangopol D (2013) A probabilistic approach for the prediction of seismic resilience of bridges. *Earthq Eng Struct Dyn* 42:1469–1487. <https://doi.org/10.1002/eqe.2282>
- Dowding CH, Rozen A (1978) Damage to rock tunnels from earthquake shaking. *J Geotech Eng Div* 104(2):175–191
- Elnashai A, Gencturk B, Kwon OS, Al-Qadi I, Hashash Y, Roesler J, Kim SJ, Jeong, SH, Dukes J, Valdivia A (2010) The Maule (Chile) earthquake of February 27, 2010. Consequence assessment and case studies. Mid-America Earthquake Center. Report No. 10-04. MAE Center, United States
- Fabozzi S, Bilotta EP, Zollo M (2018) Feasibility study of a loss-driven earthquake early warning and rapid response systems for tunnels of the Italian high-speed railway network. *Soil Dyn Earthq Eng* 112(2018):232–242. <https://doi.org/10.1016/j.soildyn.2018.05.019>
- FEMA (2011) Multi-hazard loss estimation methodology. Earthquake model. Technical manual. Federal Emergency Management Agency, United States
- Hu X, Zhou Z, Chen H, Ren Y (2020) Seismic fragility analysis of tunnels with different buried depths in a soft soil. *Sustainability* 12:892. <https://doi.org/10.3390/su12030892>
- Huang G, Qiu W, Zhang J (2017) Modelling seismic fragility of a rock mountain tunnel based on support vector machine. *Soil Dyn Earthq Eng* 102(2017):160–171. <https://doi.org/10.1016/j.soildyn.2017.09.002>
- Huang ZK, Pitilakis K, Tsinidis G, Argyroudis S, Zhang DM (2020) Seismic vulnerability of circular tunnels in soft soil deposits: the case of Shanghai metropolitan system. *Tunn Undergr Space Technol*. <https://doi.org/10.1016/j.tust.2020.103341>
- Kennedy RP, Cornell CA, Campbell RD, Kaplan S, Perla HF (1980) Probabilistic seismic safety study of an existing nuclear power plant. *Nucl Eng Des* 59(2):315–338. [https://doi.org/10.1016/0029-5493\(80\)90203-4](https://doi.org/10.1016/0029-5493(80)90203-4)
- Le TS, Huh J, Park JH (2014) Earthquake fragility assessment of the underground tunnel using an efficient SSI analysis approach. *J Appl Math Phys* 2:1073–1078. <https://doi.org/10.4236/jamp.2014.212123>
- Medina F, Yanev PI, Yanev A (2010) El terremoto de magnitud 8,8 costa afuera de la región del Maule, Chile del 27 de febrero de 2010. Resumen preliminar de los daños y recomendaciones de ingeniería. Reporte 70138. Banco Mundial, Estados Unidos (in Spanish)
- MOP (2016) Asset valuation of the national highway network. Highways Management Department (in Spanish). Ministry of Public Works, Chile
- MOP (2018) National Traffic Survey Ministry of Public Works, Chile
- MOP (2019) Quarterly reports (in Spanish). Public Works Concessions Directorate. Ministry of Public Works, Chile
- MSDF (2020) Unit cost of the national investment system. Ministry of Social Development and Family, Chile (in Spanish)
- Nazari YR, Bargi K (2012) Practical approach to fragility analysis of bridges. *Res J Appl Sci Eng Technol* 4(23):5177–5182
- Nguyen DD, Park D, Shamsheer S, Nguyen VQ, Lee TH (2019) Seismic vulnerability assessment of rectangular cut-and-cover subway tunnels. *Tunn Undergr Space Technol* 86:247–261. <https://doi.org/10.1016/j.tust.2019.01.021>
- Osmi SKC, Ahmad SM (2016) Seismic fragility curves for shallow circular tunnels under different soil conditions. *J Civ Environ Eng* 10(10):1351–1357
- Park D, Lee TH, Nguyen DD, Ahn JK (2019) Development of fragility curves for underground box tunnels from nonlinear frame analysis. In: Silvestri F, Moraci N (eds) *Earthquake geotechnical engineering for protection and development of environment and constructions—proceedings of the 7th international conference on earthquake geotechnical engineering*, pp 4371–4378
- Poulos A, Monsalve M, Zamora N, de la Llera JC (2019) An updated recurrence model for Chilean subduction seismicity and statistical validation of its Poisson nature. *Bull Seismol Soc Am* 109(1):66–74. <https://doi.org/10.1785/0120170160>
- Qiu W, Huang G, Zhou H, Xu W (2018) Seismic vulnerability analysis of rock tunnel. *Int J Geomech*. [https://doi.org/10.1061/\(ASCE\)GM.1943-5622.0001080](https://doi.org/10.1061/(ASCE)GM.1943-5622.0001080)
- Rossetto T, D'Ayala D, Ioannou I, Meslem A (2014) Evaluation of existing fragility curves. In: Pitilakis K et al (eds) *SYNER-G: typology definition and fragility functions for physical elements at seismic risk, geotechnical, geological and earthquake engineering* 27. Springer, Dordrecht, pp 47–93
- Roy N, Sarkar R (2017) A review of seismic damage of mountains tunnels and probable failure mechanisms. *Geotech Geol Eng* 35(2017):1–28. <https://doi.org/10.1007/s10706-016-0091-x>

- Scherbaum F, Kuehn N (2011) Logic tree branch weights and probabilities: summing up to one is not enough. *Earthq Spectra* 27(4):1237–1251. <https://doi.org/10.1193/1.3652744>
- Scherbaum F, Bommer J, Bungum H, Cotton F, Abrahamson NA (2005) Composite ground-motion models and logic trees: methodology, sensitivities, and uncertainties. *Bull Seismol Soc Am* 95(5):1575–1593. <https://doi.org/10.1785/0120040229>
- Selva J, Argyroudis S, Ptilakis K (2013) Impact on loss/risk assessments of inter-model variability in vulnerability analysis. *Nat Hazards* 67(2):723–746. <https://doi.org/10.1007/s11069-013-0616-z>
- Sharma S, Judd W (1991) Underground opening damage from earthquakes. *Eng Geol* 30:263–276. [https://doi.org/10.1016/0013-7952\(91\)90063-Q](https://doi.org/10.1016/0013-7952(91)90063-Q)
- Shedlock KM, Tanner JG (1999) Seismic hazard map of the western hemisphere. *Ann Geophys* 42(6):1199–1214. <https://doi.org/10.4401/ag-3779>
- Shinozuka M, Feng MQ, Lee J, Naganuma T (2000) Statistical analysis of fragility curves. *J Eng Mech* 126(12):1224–1231. [https://doi.org/10.1061/\(ASCE\)0733-9399\(2000\)126:12\(1224\)](https://doi.org/10.1061/(ASCE)0733-9399(2000)126:12(1224))
- Vanuvamalai A, Jaya KP, Balachandran V (2018) Seismic performance of tunnels structures: a case study. *Nat Hazards* 93(1):453–468. <https://doi.org/10.1007/s11069-018-3308-x>
- Wang ZZ, Zhang Z (2013) Seismic damage classification and risk assessment of mountain tunnels with a validation for the 2008 Wenchuan earthquake. *Soil Dyn Earthq Eng* 45(2013):45–55. <https://doi.org/10.1016/j.soildyn.2012.11.002>
- Wang WL, Wang TT, Su JJ, Lin CH, Seng CR, Huang TH (2001) Assessment of damage in mountains tunnels due to the Taiwan Chi-Chi earthquake. *Tunn Undergr Space Technol* 16(1):133–150. [https://doi.org/10.1016/S0886-7798\(01\)00047-5](https://doi.org/10.1016/S0886-7798(01)00047-5)
- Werner S, Taylor C, Cho S, Lavoie JP, Huyck C, Eitzel C, Chung H, Eguchi R (2006) Redars 2 methodology and software for seismic risk analysis of highway systems. Special report MCEER-07-SP08, The State University of New York, United States
- Xiaoqing F, Junqui L, Xiaolan Z, Runzhou L (2008) Damage evaluation of tunnels in earthquakes. In: 14th World conference on earthquake engineering, October 12–17, Beijing, China
- Yen WH, Chen G, Buckle I, Allen T, Alzamora D, Ger J, Arias JG (2011) Post-earthquake reconnaissance report on transportation infrastructure: impact of the February 27, 2010, Offshore Maule Earthquake in Chile. Report FHWA-HRT-11-030. Federal Highway Administration, The United States
- Zhang X, Jiang Y, Sugimoto S (2018) Seismic damage assessment of mountain tunnel: a case study on the Tawarayama tunnel due to the 2016 Kumamoto earthquake. *Tunn Undergr Space Technol* 71(2018):138–148. <https://doi.org/10.1016/j.tust.2017.07.019>

Publisher's Note Springer Nature remains neutral with regard to jurisdictional claims in published maps and institutional affiliations.